

Proximity effects and Andreev reflection in mesoscopic SNS junction with perfect NS interfaces

Z. D. Kvon,¹ T. I. Baturina,¹ R. A. Donaton,² M. R. Baklanov,^{1,2} K. Maex,² E. B. Olshanetsky,¹ A. E. Plotnikov,¹ J. C. Portal³

¹ *Institute of Semiconductor Physics, 630090, Novosibirsk, Russia*

² *IMEC, Kapeldreef 75, B-3001 Leuven, Belgium*

³ *CNRS-LCMI, F-38042, Grenoble, France*

Low temperature transport measurements on superconducting film–normal wire–superconducting film (SNS) junctions fabricated on the basis of thin superconducting polycrystalline PtSi films are reported. Due to the perfectness of SN boundaries in the junctions, zero bias resistance dip related to pair current proximity effect and subharmonic energy gap structure originating from phase coherent multiple Andreev reflections have been observed and studied.

74.76.-w, 74.80.Fp, 74.50.+r

Research activity in the study of properties of NS and SNS junctions (where N is a normal metal and S is a superconductor) has increased significantly over the past few years, mainly owing to technological advances in fabrication of mesoscopic hybrid systems. Until now, all such systems have been made by a combination of different materials, for example, the superconductor–normal metal pairs Al–Ag [1], Nb–Al and Nb–Ag [2], superconductor–heavily doped semiconductor pairs Nb– n^+ InGaAs [3], Nb– n^+ InAs [4], Nb– p^+ Si [5,6], Al– n^+ GaAs [7] and so on. One of the important topics of the physics of NS and SNS junctions is the current–voltage characteristics behavior. Two interesting phenomena can be observed from the dependence of SNS differential resistance versus bias voltage (dV/dI - V): an anomalous resistance dip at zero bias [2–7], the so-called zero bias anomaly (ZBA); and symmetrical dips at nonzero biases [7,8]. In some cases the existence of tunnel barriers at the NS interfaces does not give the possibility of the definite interpretation of experimental results.

In this paper we report the fabrication and study of SNS junctions with perfect SN interfaces. The best way to obtain a perfect junction is to have both superconducting and normal metal parts of an SNS junction made of the same material. It is known that the wires made from some thin superconducting metallic films can have the transition temperature T_c less than that of the film itself. We have used this property to fabricate the ideal SNS junctions.

We started with fabrication of ultrathin PtSi films. Smooth, continuous and uniform PtSi films with thickness of 6 nm were formed on Si substrates by deposition of a thin Pt layer followed by a rapid thermal annealing step at 450°C for 60 s to convert the as-deposited Pt into PtSi. The films formed were polycrystalline, with an average grain size of roughly 20 nm.

The samples used in the experiments are three Hall bridges with 50 μm in width and 100 μm in length. The main parameters of the films obtained from Hall measure-

ments at $T > T_c = 0.54$ K are presented in Table I. The diffusion constant is estimated assuming the simple free electron model. As is seen from Table I, our PtSi films are metal films with small mean free path. It should be noted that they have a hole type conductivity.

PtSi wires of length $L = 1.5$ μm and 6 μm and width $W = 0.3$ μm were fabricated by means of electron lithography and subsequent plasma etching and placed in one of the Hall bridges. For a schematic picture of the samples, and a scanning electron micrograph of one of the structures, see Fig. 1. At $T > T_c$ the resistances of the wires are $R_N \sim 610$ Ω for $L = 1.5$ μm and $R_N \sim 2600$ Ω for $L = 6$ μm . These values correspond to the wire sheet resistance of $R_{\square} = 120$ –130 Ω , that is slightly larger than R_{\square} of the film itself. About ten samples were investigated. None of the wires were superconducting down to $T = 35$ mK. The reason for that is not completely understood. The suppression of the superconductivity possibly results from the intrinsic stresses in the PtSi films which increase in constrictions. This suggestion is supported by the enhancement of the PtSi sheet resistance. Maybe there is another reason of the losing superconductivity in the wires. Nevertheless, after the processing we have at $T < T_c$ the SNS junctions which consist of two superconducting seas connected by the normal metal PtSi wire.

The measurements were carried out with the use of a phase sensitive detection technique at a frequency of 10 Hz that allowed us to measure the differential resistance ($R_{\text{SNS}} = dV/dI$) as a function of the dc voltage (V). The ac current was equal to 10 nA. Figure 2 shows typical dependences of dV/dI - V for the structures with (a) short ($L = 1.5$ μm) and (b) long ($L = 6.0$ μm) wires at $T = 35$ mK. Manifest zero bias resistance dip with respect to the resistance R_N at $T > T_c$ are observed, with quick initial increasing differential resistance being followed by a less steep increase at some dc bias. For SNS junctions with the short wires ($L = 1.5$ μm) a number of symmetrical features (marked as V_1 and V_2 in Fig. 2a) can be seen. It is necessary to note that the resistance

value in this bias range exceeds the wire resistance R_N at $T > T_c$. The dependences of dV/dI versus V at different temperatures are shown in Fig. 3. Both the deep minimum at zero bias and the sharp minima at nonzero biases are temperature dependent. Above T_c the features disappear. The symmetrical sharp dips at nonzero biases observed in R_{SNS} versus V (Fig. 2a and Fig. 3) are the so-called subharmonic energy gap structure (SGS) originated from the multiple Andreev reflections [9,10]. The positions of these dips are determined by the condition $V = \pm 2\Delta/en$, with $(n = 1, 2, 3, \dots)$, where Δ is the superconducting energy gap. The dips corresponding to $V = \pm 2\Delta/e$ and $\pm \Delta/e$ manifest in our case. The inset to Fig. 3 shows the temperature dependence of the positions of these dips. It actually reflects the dependence of the superconducting gap $\Delta(T)$ and strongly supports the SGS nature of the dips. The results presented above show that SGS is clearly observed even in the case of diffusive transport with very small mean free path (we have $L/l \sim 1.3 \times 10^3$ for the short wire) due to a large phase coherence length. This shows that in the SNS junctions under study the SGS is determined by phase coherent transport of retroreflected holes in the normal wire between the superconducting seas. The importance of the phase coherence to observe SGS is supported by the experiment with the long wires (Fig. 2b) where no SGS is seen. Similar results have been reported recently by Kutchinsky et al. [7] where SGS have been studied in Al- n^+ GaAs-Al mesostructures.

Figure 4 shows: (a) the superconducting transitions of the PtSi film as functions of the magnetic field at several temperatures, providing the upper critical fields at various T , and (b) the zero bias resistance for the structure with short wire under the same conditions. Three distinct regions most pronounced for the curve at the lowest temperature can be observed in Fig. 4b: (1) at the magnetic fields $B < 20$ mT, the SNS junctions exhibit a linear dependence of $R(B)$, with this feature surviving up to $T = 400$ mK; (2) there is a range of the magnetic fields where $R = R_N$; (3) a sharp rise of the resistance is resulted from the transition of the superconducting seas into a normal state. This can be seen by comparing the results presented in Fig. 4a and Fig. 4b.

The issue to be addressed now is the behavior of R_{SNS} at the zero magnetic fields and the zero bias. As one can see from Fig. 2, at the lowest temperatures the value of $\Delta R_{\text{SNS}}/R_N$ for all samples is approximately 10%, with R_{SNS} reaching R_N roughly at the same dc bias. The similar large value of extraconductance ΔG has been observed earlier in mesoscopic SNS and SN junctions [2–6].

There are different theoretical models explaining the extraconductance, ranging from pair current proximity effect to weak localization effects. These approaches are not necessarily opposed to each other, but determined by the object under study. The analysis of all these mechanisms showed that our experimental data are best

explained by the pair current proximity effect. If weak localization were the dominant mechanism [7,11–13], we should expect values of ΔG less than $10^{-6} \Omega^{-1}$ because of very small mean free path. However, in our experiments we have observed $\Delta G \sim 2.2 \times 10^{-4} \Omega^{-1}$ for the junctions with short wires and $\Delta G \sim 3.6 \times 10^{-5} \Omega^{-1}$ for those with long ones. The conventional proximity effect is known to imply that the Cooper pair amplitude decays exponentially with distance into a normal metal over the characteristic length $\xi_N = \sqrt{\hbar D/2\pi kT}$. It can effect in decrease the wire length, and resistance. In our case estimated length $\xi_N \approx 150$ nm at 35 mK, and we get extraconductance $\Delta G = 4 \times 10^{-4} \Omega^{-1}$ at $L = 1.5 \mu\text{m}$ and $\Delta G = 2 \times 10^{-5} \Omega^{-1}$ at $L = 6.0 \mu\text{m}$, which is close to ΔG experimentally observed at this temperature. We suppose it is the suppression of the proximity effect that is responsible for reaching R_N on the dependences of dV/dI - V (Fig. 2) and weak plateau on the magnetic field dependences (Fig. 4). Similar plateaus on the dV/dI - B curves were observed in Ref. [2]. The following increase of the differential resistance may be connected with the penetration of the normal state into the superconducting region. This phenomenon, that was theoretically predicted by Geshkenbein et al. [14], implies that if the transition temperature changes slowly with a distance near an SN interface at some value of the current the penetration of the electrical field into superconductor occurs. This is likely to be our case, as the reasons leading to the suppression of the superconductivity in the wires may produce the transitional region with varying order parameter.

In summary, we have observed for the first time the large ZBA and SGS in perfect SNS junctions in the regime of diffusive transport. To compare, ZBA was observed without SGS in Ref. [2–6]. On the other hand, van Huffelen *et al.* [8] saw SGS in their samples, but no ZBA. There is the only paper [7] where ZBA and SGS occur in the same junction, but this ZBA is quite different and more complicated than the one observed by us. At the lowest temperature a weak ZBA (1%–5%) occurred at low bias ($V < 100 \mu\text{V}$), it disappeared together with SGS when the temperature increased, and after that a new wider ZBA arose. The difference in the behavior of the junctions can be related to the quality of NS interfaces. There is no guarantee that any kind of barrier is absent between the superconductor and the normal metal or the semiconductor in the above references. The results of our paper strongly support the fact that ZBA and SGS can be observed in SNS junctions with a perfect NS interface.

We are grateful to S. N. Artemenko, E. G. Batyev and M. V. Entin for helpful discussions. This work has been supported by EU program PHANTOMS and by grant No. 5-4 of the program “Physics of quantum and wave processes” of the Russian Ministry of Science and Technology.

-
- [1] V. N. Petrashov, V. N. Antonov, P. Delsing and R. Claesson, *Phys. Rev. Lett.* **70**, 347 (1993).
- [2] P. Xiong, G. Xiao and R. B. Laibowitz, *Phys. Rev. Lett.* **71**, 1907 (1993).
- [3] A. Kastalsky, A. W. Kleinsasser, L. H. Greene, R. Bhat, F. P. Milliken, and J. P. Harbison, *Phys. Rev. Lett.* **67**, 3026 (1991).
- [4] C. Nguyen, H. Kroemer and E. Hu, *Phys. Rev. Lett.* **69**, 2847 (1992).
- [5] P. H. C. Magnee, N. van der Post, P. H. M. Koostra, B. J. van Wees, and T. M. Klapwijk, *Phys. Rev. B* **50**, 4594, (1994).
- [6] T. M. Klapwijk, *Physica B* **197**, 481 (1994).
- [7] J. Kutchinsky, R. Taborski, T. Clausen, C. B. Sorensen, A. Kristensen, P. E. Lindelof, J. Bindslev Hansen, C. S. Jacobsen, and J. L. Skov, *Phys. Rev. Lett.* **78**, 931 (1997).
- [8] W. M. van Huffelen, T. M. Klapwijk, D. R. Heslinga, M. J. de Boer, and N. van der Post, *Phys. Rev. B* **47**, 5170 (1993).
- [9] M. Octavio, M. Tinkham, G. E. Blonder, and T. M. Klapwijk, *Phys. Rev. B* **27**, 6739 (1983).
- [10] K. Flensberg, J. Bindslev Hansen, M. Octavio, *Phys. Rev. B* **38**, 8707 (1988).
- [11] B. J. van Wees, P. de Vries, P. Magnee, and T. M. Klapwijk, *Phys. Rev. Lett.* **69**, 510 (1992).
- [12] C. W. J. Beenakker, *Phys. Rev. B* **46**, 12841 (1992).
- [13] I. K. Marmorosk, C. W. J. Beenakker, R. A. Jalabert, *Phys. Rev. B* **48**, 2811 (1993).
- [14] V. B. Geshkenbein, A. V. Sokol, *Zh. Eksp. Teor. Fiz.* **94**, 259 (1988) [*Sov. Phys. JETP* **67**, 362 (1988)].

TABLE I. The basic parameters of the PtSi films obtained from Hall measurements at $T > T_c = 0.54$ K and physical quantities deduced from them (mean free path l , elastic scattering time τ and diffusion constant D).

d	R_{\square}	n	τ	$k_F l$	D	l
(nm)	(Ω)	(cm^{-3})	(s)		(cm^2/s)	(nm)
6	104	$7 \cdot 10^{22}$	$8 \cdot 10^{-16}$	15	6	1.2

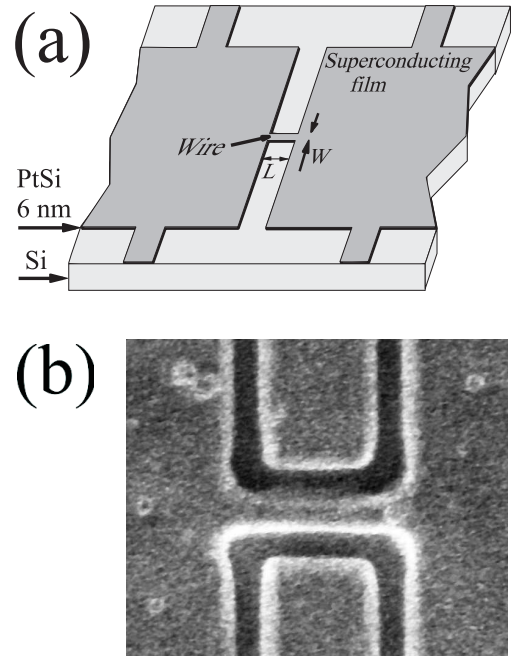


FIG. 1. (a) Schematic view of a junction. (b) SEM image of the PtSi wire with length $1.5 \mu\text{m}$ and width $0.3 \mu\text{m}$ formed by electron beam lithography and subsequent plasma etching.

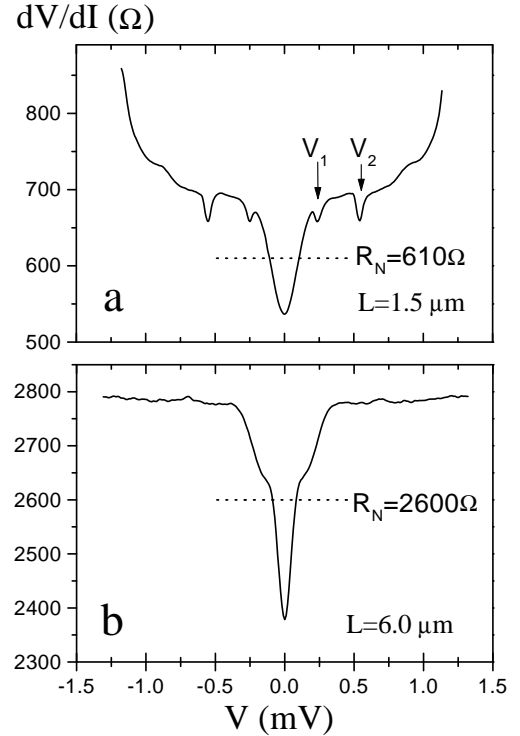


FIG. 2. Differential resistance versus dc bias voltage for two samples with the same width $W = 0.3 \mu\text{m}$ and different lengths (a) $L = 1.5 \mu\text{m}$ and (b) $L = 6.0 \mu\text{m}$, measured at $T = 35$ mK.

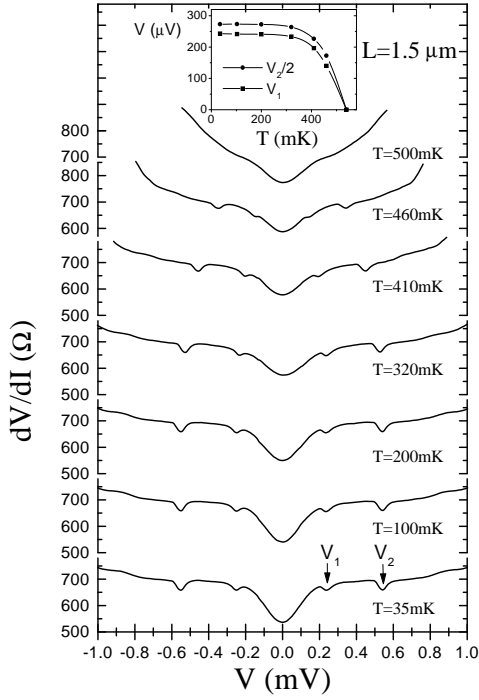


FIG. 3. Differential resistance of the sample with $1.5 \mu\text{m}$ wire length as a function of bias voltage at different temperatures showing a zero bias resistance dip and symmetrical dips marked as V_1 and V_2 on the lower curve. Inset: Voltage positions of the resistance dips as a function of temperature.

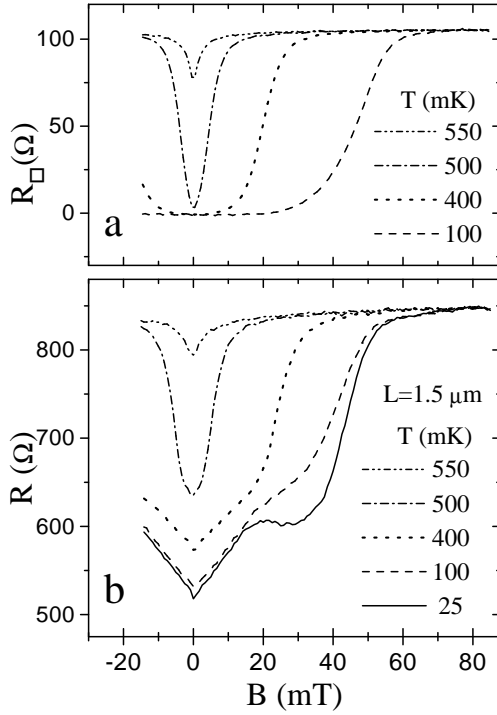


FIG. 4. (a) The magnetic field dependences of the sheet resistance of the 6 nm thick PtSi film measured at several temperatures. (b) The zero bias resistance of the sample with $1.5 \mu\text{m}$ wire length under the same conditions.